



Decrease of Material Burden in a Novel Alkali-Saving Reduction Treatment Process of Nickel Slag Based on NaOH Roasting

HAI-YANG LIU,^{1,2} NAN XIANG,^{2,3} XIAO-YI SHEN,¹ YU-CHUN ZHAI,¹
and CHAO HAN²

1.—School of Metallurgy, Northeastern University, Shenyang 110819, China. 2.—School of Materials Science and Engineering, Henan University of Science and Technology, Luoyang 471000, China. 3.—e-mail: xiangnan-87@163.com

Conventional reduction treatment methods for nickel slag show drawbacks such as high energy cost, heavy material burden or secondary pollution. Thus, a novel environmentally friendly reduction treatment method for high-silicon wastes, especially nickel slag, is proposed in this paper. The main characteristic is to lower the alkali-ore ratio (mass ratio of NaOH to ore) through introducing a high-speed premixing procedure before roasting. Optimal process parameters have been found experimentally, i.e., a roasting temperature of 823 K, alkali-ore ratio of 1.6:1, and roasting time of 30 min. The desilication ratio reached to 91.3 wt.%. Compared with previous NaOH roasting processes with stirring, the NaOH consumption is down by 60%, which greatly reduces the material burden. Through carbonation decomposition of the Na_2SiO_3 solution generated in the NaOH roasting, amorphous silica is recycled as the final product. The proposed method is expected to be a promising method for industrial reduction treatment of nickel slag.

INTRODUCTION

The development of the nickel extraction industry leads to the continuous accumulation of nickel slag. Traditional disposition methods, such as simple landfill, seriously pollute soil and underground water. In addition, the useful and valuable silicon resources in nickel slag are wasted. As a result, the reduction treatment of nickel slag not only meets the urgent requirement of environment protection but also recycles an important raw material (i.e., silica).

The main reduction treatment methods of high-silicon wastes such as nickel slag are commonly alkali leaching and alkali roasting. The principle is to separate the silicon from the high-silicon wastes and convert it into available products containing silicon. NaOH solution was used to decompose the high-silicon wastes in the alkali leaching process, and Na_2CO_3 or NaOH was used as the alkali source in the alkali roasting process.

The key procedure of alkali leaching is the activation pretreatment of high-silicon wastes. The activation pretreatment techniques include thermal activation, mechanical activation and acid

activation.^{1–3} Gao et al.¹ roasted coal gangue at 1273 K for 2 h, and then completed the reduction by alkali leaching. Yang et al.² and Mu et al.⁴ also used thermal activation to pretreat high-silicon wastes. Thermal activation can convert inert silica in the form of silicate into free active silica, which is convenient for the subsequent reduction of high-silica wastes by alkali leaching. Obviously, thermal activation can increase the content of the active silica and the reactivity of the materials, but the disadvantage is that high-temperature calcination will lead to high energy consumption. Li et al.⁵ used a planetary ball mill to grind and mix fly ash and CaCO_3 for 2 h. Then, mesoporous silica was prepared by calcification, acid leaching and filtration, and the reduction of fly ash was completed. Mechanical activation can transform macro-mechanical energy into micro-activation energy, and simultaneously mix the materials evenly, which provides good conditions for subsequent chemical reactions.^{6,7} The advantage of mechanical activation is that it does not need high temperatures, but its disadvantage is the long grinding time and the low efficiency of the mechanical energy conversion.^{8,9} Fedoročková et al. activated serpentine with HCl at

333 K, and obtained raw material with a high activity of silica. Then, amorphous silica was prepared by alkali leaching and acidification. Strong acid removes metal ions from inert silicates and converts them into free active silica, which provides the reaction conditions for alkali leaching.¹⁰ The advantage of acid activation is the high activation efficiency, but it produces a large amount of low-acid wastewater which is difficult to treat.^{11,12} In summary, the activation pretreatment of high-silicon wastes commonly leads to complicated process routines, large energy consumption or a large amount of low-acid wastewater which is difficult to dispose.

Another reduction treatment method, alkali roasting, does not need activation pretreatment,^{13,14} and may avoid the drawbacks caused by such a process. It can be divided into Na₂CO₃ roasting and NaOH roasting. Mermer et al. used Na₂CO₃ as the alkali source to roast fly ash at 1163 K for 3 h for reduction.¹⁵ At the roasting temperature, molten Na₂CO₃ can infiltrate into the high-silicon waste, accelerate the roasting reaction process and shorten the reaction time. However, the energy consumption of high-temperature roasting for a long time is very high.^{16,17} Kongnoo et al. used the NaOH roasting method to desilicate palm oil ash residue at 873 K for 1 h to achieve reduction.¹⁸ Compared with the Na₂CO₃ roasting method, this method has the advantages of low roasting temperatures and short roasting times, so it is more suitable for the reduction of high-silicon wastes, but the roasting time is still more than 1 h, and the energy consumption is still high. Mu et al. introduced stirring into the roasting process to further shorten the roasting time (only 20 min) of nickel laterite ore.⁴ The results showed that the desilication ratio reached 93.4 wt.% in a roasting time of 20 min, roasting temperature of 823 K, alkali-ore ratio (mass ratio of NaOH to ore) of 4:1 and stirring speed of 400 rpm. The disadvantages are the high alkali-ore ratio, a heavy burden of materials, serious environmental pollution and the need for a stainless steel reactor with an agitator. If the NaOH consumption can be further reduced, its material burden can be lowered, which may accelerate the further application of this method.

On the basis of the NaOH roasting process with stirring proposed by Mu et al.,⁴ a novel environmentally friendly reduction technology for high-silicon wastes, especially nickel slag, is proposed in this paper, which avoids stirring in the roasting process, and lowers the NaOH consumption through introducing a high-speed premixing procedure for the reactive materials before roasting. The premixing procedure can make the reaction materials mix more evenly before roasting, thus ensuring that the molten NaOH can completely infiltrate the high-silicon waste in a short enough time, so as to shorten the roasting time. In this way, the advan-

tages of the process proposed by Mu et al.⁴ can be maintained, the NaOH consumption is also cut down, while the modulus of the Na₂SiO₃ solution increases. Then, the material burden in the whole process is ultimately decreased and environmental pollution is alleviated.

In detail, this paper first studies the effect of alkali-saving NaOH roasting on the reduction treatment of nickel slag, and optimizes the roasting process parameters (as shown in Table I). In addition, the process parameters of carbonation decomposition for preparing amorphous silica were optimized (as shown in Table I). The micro-morphology, phase analysis and chemical composition of the samples are given.

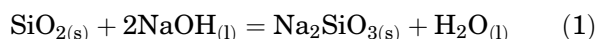
OVERVIEW OF THE PROPOSED METHOD

Reduction Process

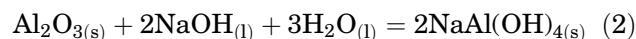
The proposed process for nickel slag reduction treatment is compared with Mu et al.'s process,⁴ as shown in Fig. 1. Figure 1a shows that the desilication ratio of Mu et al.'s process reaches 93.4 wt.% at the roasting time of 20 min, the roasting temperature of 823 K, the alkali-ore ratio of 4:1 and the stirring speed of 400 rpm. Figure 1b shows that the desilication ratio of the proposed process reaches 91.3 wt.% at the premixing time of 120 s, the roasting temperature of 823 K, the roasting time of 20 min and the alkali-ore ratio 1.6:1. Obviously, the alkali-ore ratio decreased by 60% (which will be confirmed below), and therefore the material burden of the reduction process is greatly reduced. Meanwhile, the advantages of Mu et al.'s process are properly maintained.

Principle

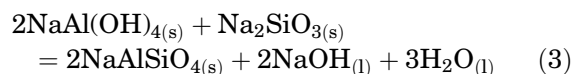
The main reaction of desilication by NaOH roasting is the formation of Na₂SiO₃, as shown in Eq. 1.⁴



Because the nickel slag contains a small amount of alumina, the reaction produces NaAl(OH)₄, as shown in Eq. 2.¹⁹



At the same time, the formation reaction of undissolved nepheline follows, as shown in Eq. 3.¹⁹



The formation of nepheline makes part of the dissolved silica return to the slag and reduces the desilication ratio, which is a major obstacle to improving the reduction effect. Therefore, in order to improve the reduction effect, the formation of nepheline must be prevented.^{20,21}

Table I. Chemical components of the samples and experimental conditions

Chemical components of the samples (wt.%)						
	SiO ₂	Fe ₂ O ₃	Al ₂ O ₃	MgO	K ₂ O	CaO
Nickel slag	70.43	7.91	2.33	3.74	0.88	0.42
Desilication residue	17.65	22.03	3.38	10.41	1.67	1.17
Amorphous silica	99.92	0.008	0.001	–	–	<0.001

Experimental preparation of sodium silicate solution

Premixing time (s) ^a	Roasting temperature (K) ^b	Roasting time (min) ^c	Alkali-ore ratio (wt/wt) ^d
20, 40, 60, 80, 100, 120, 140, 160	573, 623, 673, 723, 773, 823, 873, 923	5, 15, 30, 45, 60, 90, 100	0.8, 1.0, 1.2, 1.4, 1.6, 1.8, 2.0

Experimental preparation of amorphous silica

Carbonation decomposition time (min) ^e	Gas flow rate (ml/min) ^f	Stirring speed (rpm) ^g	Temperature (K) ^h
0–270, sampling every 30 min (for Na ₂ CO ₃ concentrate), and sampling every 5 min (for pH measurement)	20, 30, 40, 50, 60, 70, 80	250, 300, 350, 400, 450, 500, 550, 600	313, 323, 333, 343, 353, 363

^aRoasting temperature 823 K, roasting time 20 min and alkali-ore ratio 1:1. ^bPremixing time 120 s, roasting time 20 min and alkali-ore ratio 1:1. ^cPremixing time 120 s, roasting temperature 823 K and roasting time 30 min. ^dGas flow rate 60 ml/min, stirring speed 400 rpm and temperature 333 K. ^epH₁ (first-step end point pH), pH₂ (second-step end point pH), stirring speed 400 rpm and temperature 333 K. ^fpH₁, pH₂, gas flow rate 80 ml/min and temperature 333 K. ^gpH₁, pH₂, gas flow rate 80 ml/min and stirring speed 450 rpm.

EXPERIMENT**Materials**

The experimental material is nickel slag supplied by a factory in Western Sichuan Province, China. An optical photograph, micromorphology and phase analysis are shown in Fig. 2a, b and c, respectively.

The mass fraction of silica in nickel slag is as high as 70.43 wt.%, which is the main component, while Fe₂O₃ and Al₂O₃ are the secondary components, the mass fraction is less than 10.00 wt.%, CaO and K₂O are lesser components, and the mass fraction is less than 1.00 wt.%, as shown in Table I. Obviously, the recovery and utilization of silica is the key to realizing the reduction treatment of nickel slag.

Figure 2a is an optical photograph of the nickel slag, which shows gray powder and the agglomeration of particles.

Figure 2b shows the SEM image of the nickel slag, from which it can be seen that the nickel slag is mainly composed of large and medium particles, mainly silica, with a small amount of talc. Mineral particles are irregular in shape, rough and fragmented in surface, and easy to fully contact with the molten alkali in the NaOH roasting.

Figure 2c shows the XRD pattern of the nickel slag, from which it can be seen that the main phase is quartz, followed by jarosite, and a small amount of talc and serpentine. These minerals can react with NaOH, in which silicon and some aluminum elements enter the Na₂SiO₃ solution, while the rest nearly all enter the desilication residue.

Solid sodium hydroxide is industrial grade with a purity of 96.0 wt.%.

Experimental Devices and Instruments

A corundum crucible (outer diameter 26 mm, inner diameter 20 mm, height 90 mm) was used as the reactor, and a box muffle furnace (SX2-2S-10g/t ± 2 K) as the roaster. The premixing of the nickel slag and solid sodium hydroxide is completed by a high-speed cutter grinder (XL-10B; 20,000 rpm).

The samples were characterized by XRD (Rigaku; goniometer accuracy < 0.0001°) and SEM (Shimadzu; resolution 3.5 nm). The chemical compositions of the samples were analyzed by ICP-OES (USPE; detection limit 0.01 μg/ml). The sample was weighed by an electronic balance (FA2004, ± 0.0002 g).

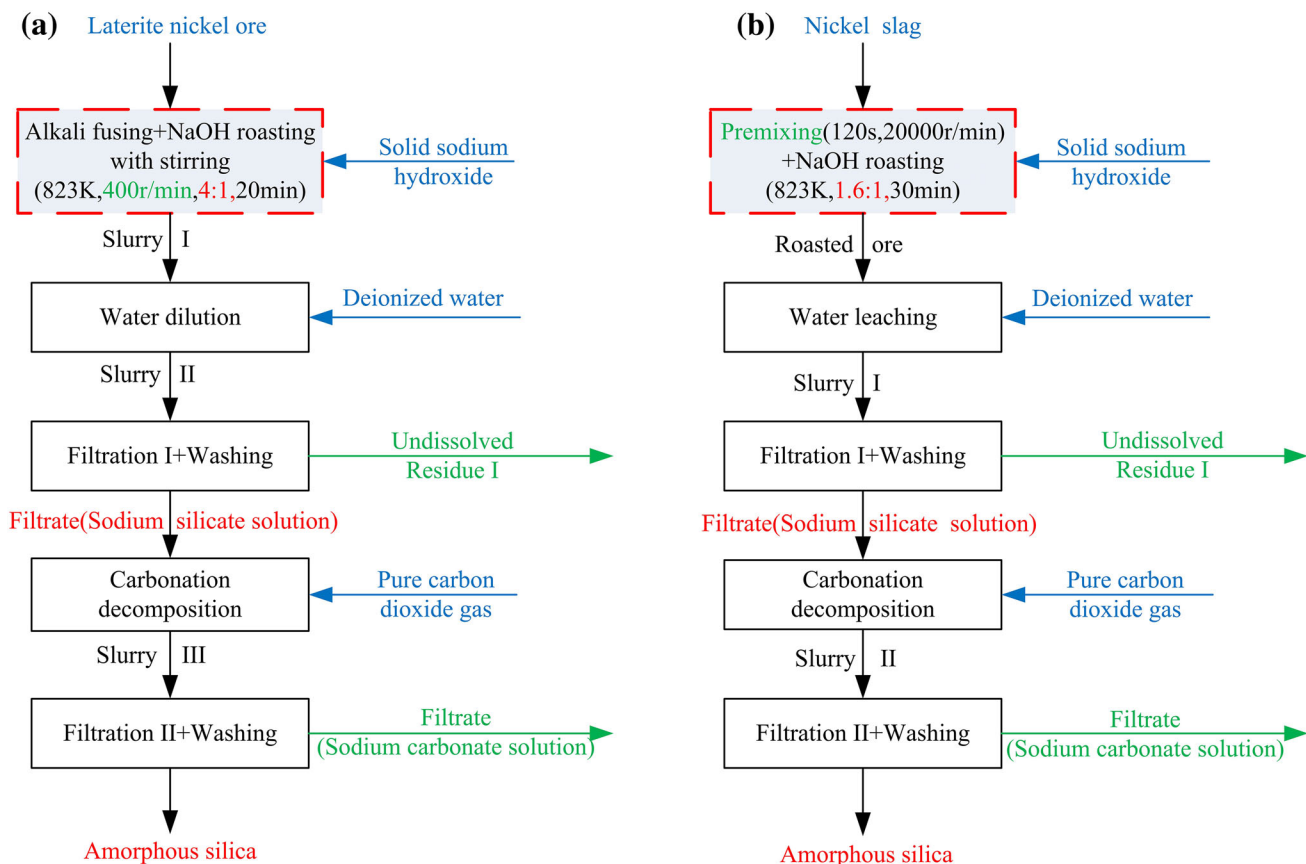


Fig. 1. Reduction process proposed by Mu et al.⁴ (a) and the novel reduction process proposed in this paper (b).

Experiment Schemes

The Preparation of Sodium Silicate Solution

The nickel slag was dried at 363 K for 24 h. According to the determined alkali-ore ratio, nickel slag and a certain quality of solid sodium hydroxide were weighed and mixed in a high-speed cutting mill. After 120 s, the premixed ore was taken out for a reserve. An electronic balance was used to weigh 71.5 g of the premixed ore which was placed into a crucible. When the muffle furnace reached the roasting temperature, the crucible was inserted. After 10 min, when the reaction material had risen to the roasting temperature, the timing began. When the roasting time was finished, the crucible was immediately taken out and air-cooled. The roasted ore was fully dissolved with 363 K deionized water, and the slurry vacuum-filtered while hot. The filtrate was cooled to room temperature with a constant volume of 500 ml for inspection.

After the NaOH roasting, the desilication effect of nickel slag can be expressed by the desilication ratio, as shown in Eq. 4.

$$\alpha = (1 - m'_{\text{SiO}_2}/m_{\text{SiO}_2}) \times 100\% \quad (4)$$

Where α is the desilication ratio of nickel slag, m'_{SiO_2} is the weight of silica in the desilication residue, and m_{SiO_2} is the weight of silica in the nickel slag.

The reduction effect of the nickel slag is expressed by the weight reduction ratio of the slag, which can be calculated by the desilication ratio of the slag, as shown in Eq. 5.

$$\beta = \alpha \times 70.43\% \times 100\% \quad (5)$$

Where β is the weight loss ratio of the slag, and α is the desilication ratio of the slag; 70.43% is the mass fraction of silica in the slag.

The Preparation of Amorphous Silica

At present, the final products of high-silicon waste by reduction treatment include mesoporous silica,²²⁻²⁴ molecular sieve,^{25,26} aerogel,²⁷⁻²⁹ amorphous silica³⁰⁻³² and so on. These products are prepared by the sol-gel process except for the amorphous silica, which requires expensive equipment, a complex process, a high cost and is difficult to put into practical production. Only amorphous silica is very likely to be put into production.

Carbon dioxide was introduced into the Na_2SiO_3 solution in a two-step method to prepare the amorphous silica. The first step is to remove impurity metal ions such as Fe^{3+} , Mg^{2+} , Mn^{2+} and Zn^{2+} , and the second step is to obtain pure amorphous silica.⁴ The detailed principle and steps can be found in Appendix I in the supplementary data file.

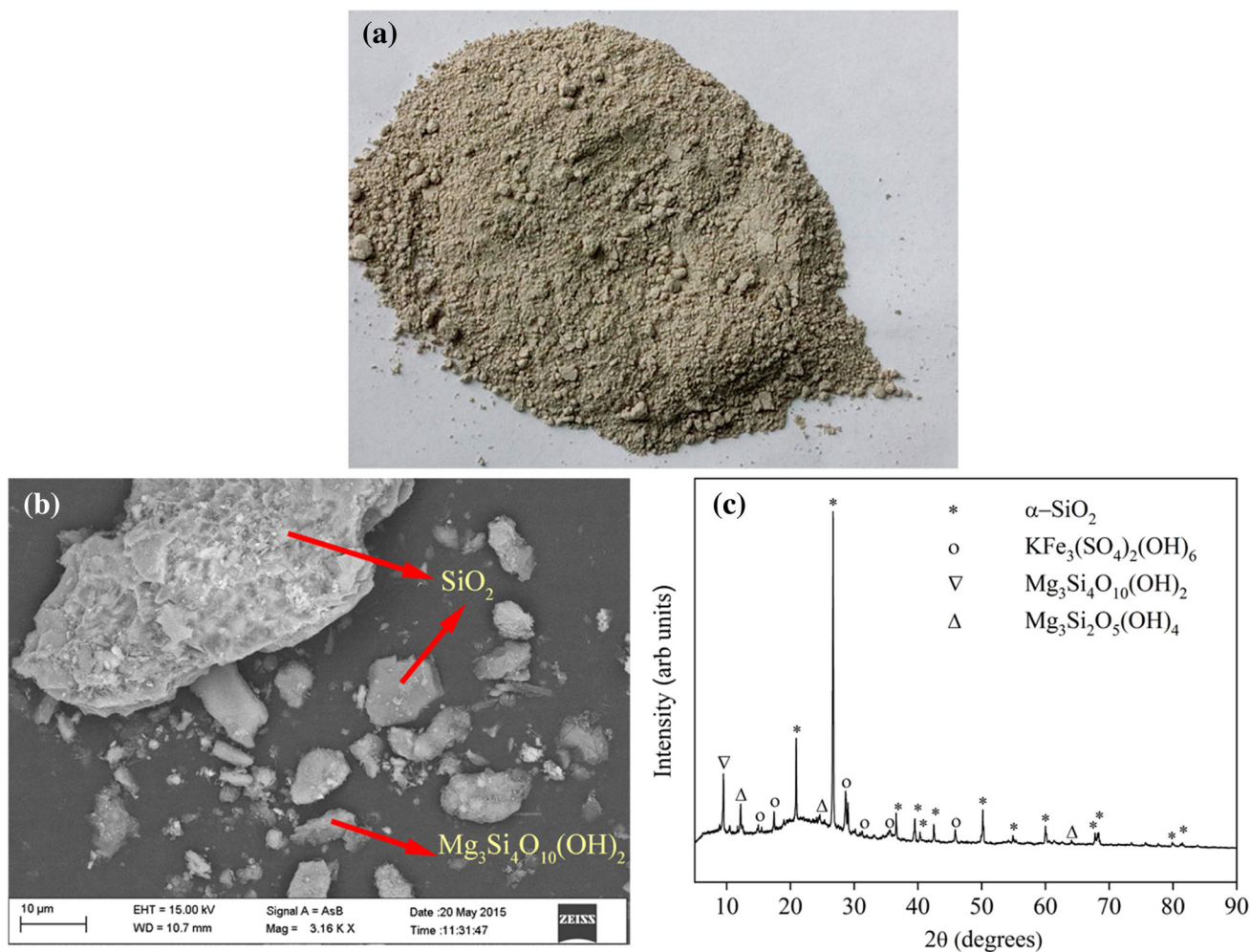


Fig. 2. Optical photograph (a), SEM image (b) and XRD pattern (c) of the nickel slag.

The experimental device mainly includes a carbon dioxide cylinder, a micro-capillary gas flow-meter, a reactor, and so on (see Supplementary Fig. S1 in detail).

RESULTS AND DISCUSSION

Effect of Roasting Parameters on the Weight Loss Ratio of Nickel Slag

Effect of Premixing Time on the Weight Loss Ratio of Nickel Slag

Figure 3a shows the effect of the premixing time on the weight loss ratio of nickel slag in the condition shown by superscript 'a' in Table I. Obviously, the weight loss ratio of nickel slag increases from 35.8% at 20 s to 52.9% at 120 s with the increase of premixing time, and then stays almost constant. The reason is that the increase of premixing time can make the mixing of the reactants more uniform, increase the contact area, and increase the reaction rate. However, after 120 s, the material

has been mixed uniformly, and the continuous increase of premixing time no longer plays a role in the reduction of the nickel slag. Hence, the optimum premixing time was set as 120 s in the condition shown by superscript 'a' in Table I.

Effect of Roasting Temperature on Weight Loss Ratio of Nickel Slag

Figure 3b shows the effect of roasting temperature on the weight loss ratio of nickel slag in the condition shown by superscript 'b' in Table I, where it is shown that the weight loss ratio of nickel slag increased from 45.2% at 573 K to 53.0% at 823 K, and then decreased to 51.6% at 923 K. The reason is that a higher temperature can increase the rate of the chemical reaction. However, when the temperature exceeds 823 K, nepheline formation as shown in Eq. 3 occurs, so that the weight loss ratio of nickel slag begins to decrease. Therefore, the optimum roasting temperature is 823 K in the condition shown by superscript 'b' in Table I.

Effect of Roasting Time on Weight Loss Ratio of Nickel Slag

Figure 3c shows the effect of roasting time on the weight loss ratio of nickel slag in the condition shown by superscript 'c' in Table I, where it is shown that the weight loss ratio increases from 48.1% at 5 min to 56.1% at 30 min. After 30 min, the weight loss ratio began to decline slowly to 54.9% at 90 min. After 90 min, the weight loss ratio did not vary. With the increase of roasting time, the silica in the nickel slag is consumed continuously with the formation of sodium silicate (Eq. 1), and the weight loss ratio of the nickel slag increases. When the roasting time exceeds 30 min, nepheline begins to form in the system (Eq. 2). Some sodium silicate is returned to the nickel slag in the form of nepheline, and the weight loss ratio of the nickel slag decreases accordingly. When the roasting time reaches 90 min, the alumina which can react with sodium silicate to form nepheline in the nickel slag is consumed completely and the quantity of sodium

silicate is no longer reduced, so the weight loss ratio of the nickel slag is no longer reduced. Therefore, the optimum roasting time is 30 min in the condition shown by superscript 'c' in Table I.

Effect of Alkali-Ore Ratio on Weight Loss Ratio of Nickel Slag

Figure 3d shows the effect of alkali-ore ratio on weight loss ratio of nickel slag in the condition shown by superscript 'd' in Table I, where it is shown that the weight loss ratio of nickel slag increases from 45.9% at 0.8:1 to 64.1% at 1.6:1 with the increase of the alkali-ore ratio, and then remains basically unvaried. With the increase of the alkali-ore ratio, the excess coefficient of alkali is larger and the chemical reaction rate is higher. However, when the alkali-ore ratio exceeds 1.6:1, enough alkali can keep the chemical reaction at the maximum rate throughout the reaction process, and it is meaningless to increase the alkali-ore ratio.

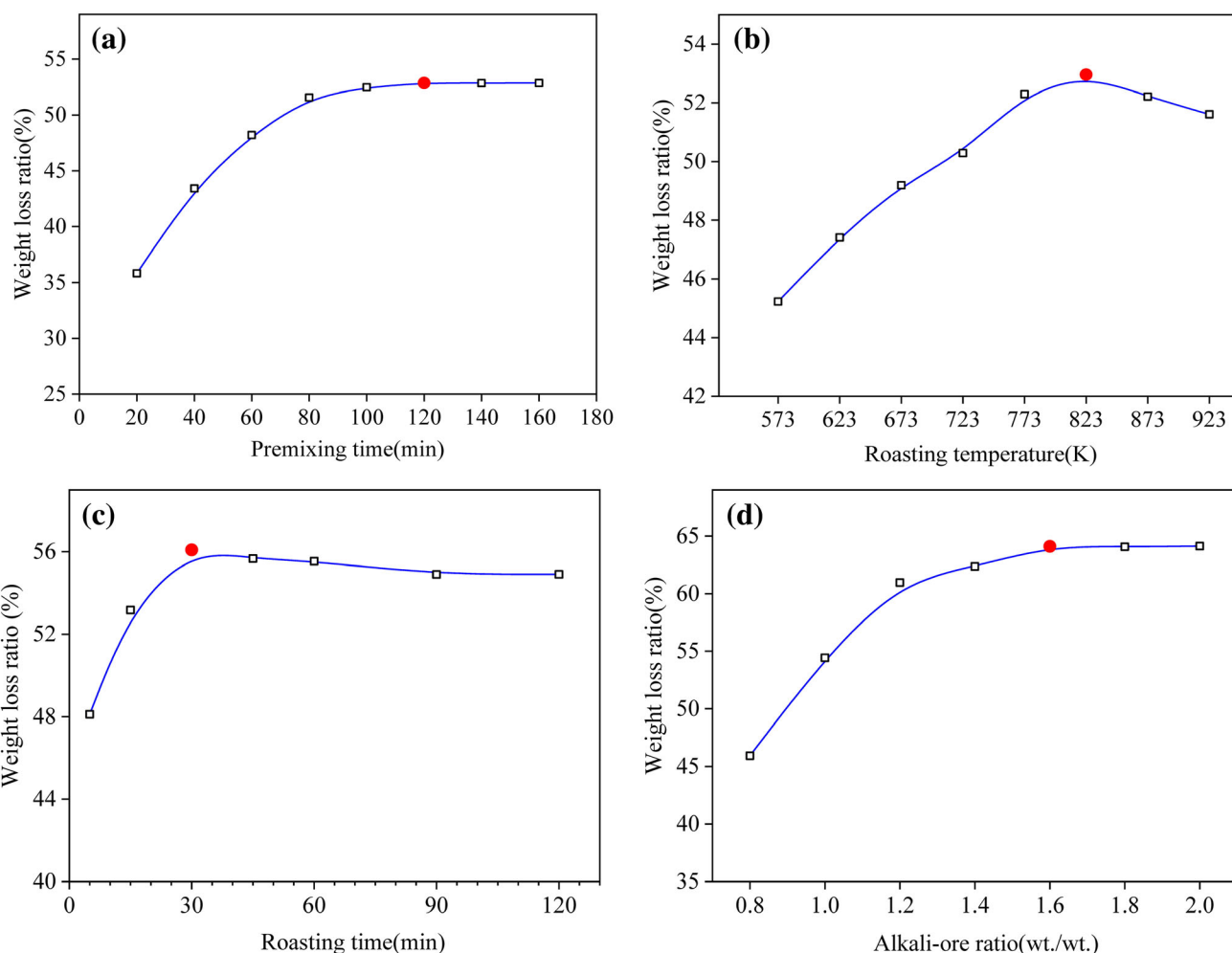


Fig. 3. Effects of premixing time (a), roasting temperature (b), roasting time (c) and alkali-ore ratio (d) on the weight loss ratio of nickel slag.

The optimum alkali–ore ratio is 1.6:1 in the condition shown by superscript ‘d’ in Table I.

Compared with Mu et al.’s method, the percentage of alkali saving in the proposed method is about 60%. As the reason behind this, Mu et al. introduced stirring into the roasting process, which ensured the full and uniform mixing of the solid and liquid materials, which greatly shortened the roasting time, but the alkali–ore ratio increases rapidly in this case. The reason is summarized as follows: firstly, for the stirring step, the semifluid of alkali and ore cannot form when the alkali–ore ratio is lower than 3:1; and secondly, the optimal desilication ratio can only be reached when the alkali–ore ratio approximates to 4:1. Therefore, it is inevitable that the alkali–ore ratio is greater than 3:1. In brief, the higher alkali–ore ratio of Mu et al.’s method is determined by the characteristics of this process.

In contrast, the proposed method avoids stirring in the roasting process, and then the higher alkali–ore ratio is no longer necessary. The premixing procedure before roasting is implemented to achieve the full and uniform contact between the solid and liquid materials, which retains the advantages of Mu et al.’s method. In this case, the full reaction between the alkali and the ore occurs in a lower alkali–ore ratio. This is verified by the experimental results, i.e. the alkali–ore ratio of the proposed method is only 1.6:1, which is dramatically lower than in Mu et al.’s work.

As for the energy consumption, 20 min of stirring of solid ore and molten alkali at elevated temperature is conducted in Mu et al.’s work, but 30 min of roasting without stirring and 2 min of premixing at room temperature are performed in this work. Meanwhile, the weight of the roasting materials in Mu et al.’s method reached 1.9 times that of the proposed method, and the energy consumption is inevitably higher. Afterwards, in each step of the process, the energy consumption increases correspondingly. Hence, the energy consumption of the proposed method is not higher than Mu et al.’s work in regard to the engineering experience.

In order to clarify the interaction between the roasting temperature, the roasting time, the roasting temperature and the alkali–ore ratio, an orthogonal experiment (see Appendix II in the supplementary file data) was carried out. The schemes of the orthogonal experiments are presented in supplementary Tables S1 and S2, and the experimental results are listed in supplementary Table S3. The results showed that there was no interaction between the roasting temperature and the roasting time, but there was a negative correlation between the roasting temperature and the alkali–ore ratio (see supplementary Fig. S2).

Na_2SiO_3 solution (modulus 0.46, silica 46 g/L) was extracted from the nickel slag by NaOH roasting, and was used as the raw feed solution for preparing amorphous silica.

Effect of Process Parameters on Carbonation Decomposition Time

Variation of Chemical Composition and pH of Feed Solution During Carbonation Decomposition

Figure 4a shows the variations of chemical composition and pH of the feed solution during carbonation decomposition in the condition shown by superscript ‘e’ in Table I. The concentration of sodium carbonate first increases and then decreases, with a maximum value of 68.34 g/L at 125 min, while the corresponding pH is 9.95. At this time, the free alkali in the feed solution completely transforms into sodium carbonate, the impurity metal ions completely precipitate, and the primary carbonation decomposition ends. The concentration of sodium carbonate dropped to 3.66 g/L at 275 min, which was the same as before the carbonation decomposition. At this time, the corresponding pH was 8.05, and the secondary carbonation decomposition ended. The pH_1 was 9.95, and the pH_2 was 8.05.

Effect of gas Flow Rate of Carbon Dioxide on Carbonation Decomposition Time

Figure 4b shows the effect of the gas flow rate of carbon dioxide on the carbonation decomposition time in the condition shown by superscript ‘f’ in Table I. With the increase of the gas flow rate, the carbonation decomposition time of the first step decreases from 630 min at 20 ml/min to 107 min at 80 ml/min. When the gas flow rate exceeds 80 ml/min, the feed solution forms a gel. The second step is similar to the first. Thus, the optimum gas flow rate is 80 ml/min in the condition shown by superscript ‘f’ in Table I.

Effect of Stirring Speed on Carbonation Decomposition Time

Figure 4c shows the effect of stirring speed on the carbonation decomposition time in the condition shown by superscript ‘g’ in Table I. With the increase of the stirring speed, the carbonation decomposition time of the first step is shortened from 174 min at 250 rpm to 140 min at 450 rpm, and then does not vary. The second step is similar to the first. Therefore, the optimum stirring speed is 450 rpm in the condition shown by superscript ‘g’ in Table I.

Effect of Temperature on Carbonation Decomposition Time

Figure 4d shows the effect of temperature on the carbonation decomposition time in the condition shown by superscript ‘h’ in Table I. With the increase of temperature, the carbonation decomposition time of the first step first decreases and then increases, while at its lowest point it is at 333 K and 343 K, the same as after 125 min. The carbonation

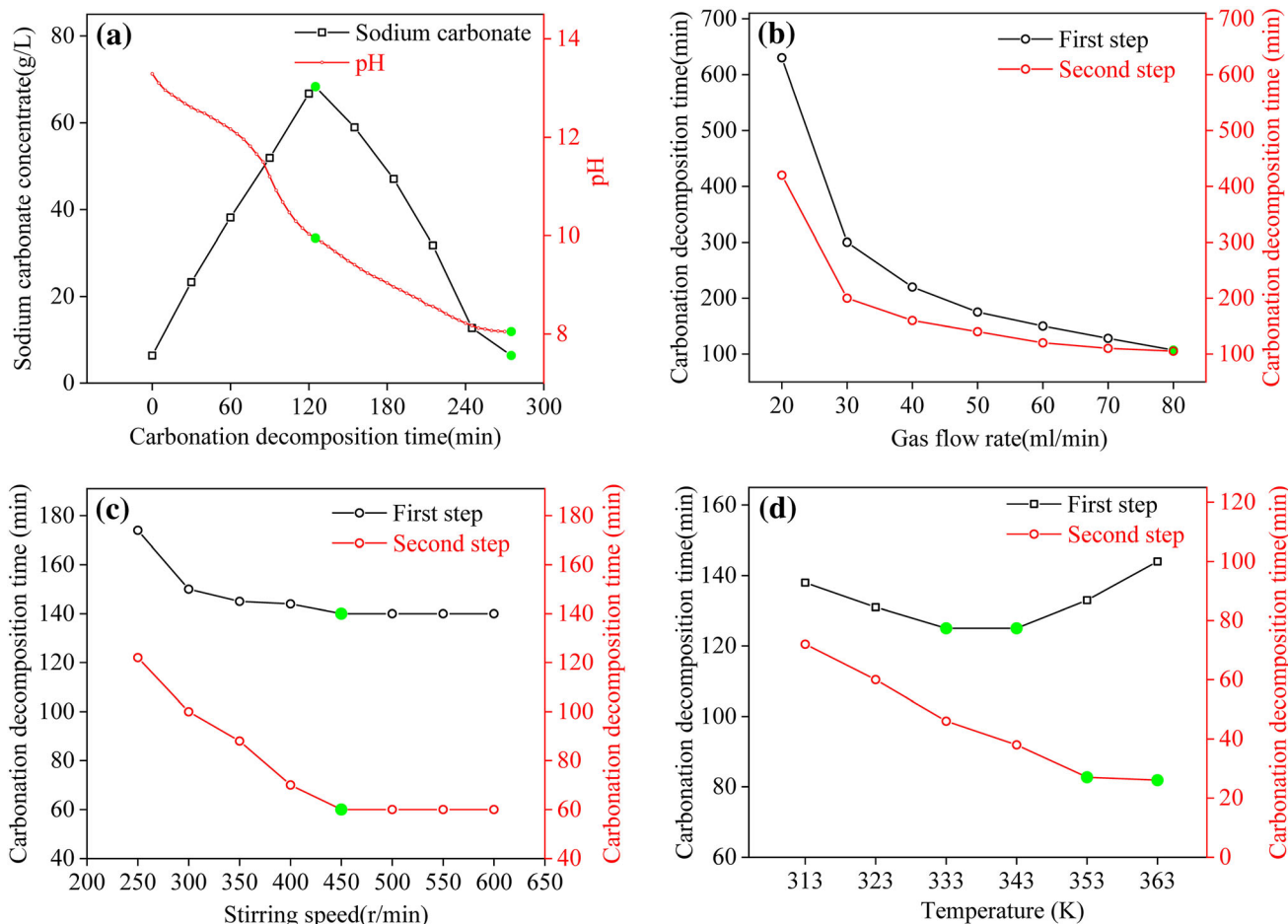


Fig. 4. Variation of chemical composition and pH of the feed solution during carbonation decomposition (a), effects of gas flow rate of carbon dioxide (b), stirring speed (c) and temperature (d) on the time of carbonation decomposition.

decomposition time of the second step decreases with the increase of temperature until 27 min at 353 K, and then no longer decreases. Therefore, in the condition shown by superscript 'h' in Table I, the optimum temperature for the first step is 333 K, while the optimum temperature for the second step is 353 K.

The amorphous silica was prepared by the two-step carbonation decomposition process, and its chemical composition is shown in Table I.

Variation of Microstructure of Nickel Slag During reduction Treatment

Figure 5a shows the micro-morphology of the nickel slag. The main component of the slag is silica, which contains a small amount of talc. The mineral particles are mainly large- and medium-sized, irregular in shape, and rough and fragmented in surface. After NaOH roasting treatment, silica and talc in the slag were removed and roasted ore was formed, mainly Na_2SiO_3 , as shown in Fig. 5b. The roasted ore particles are long and columnar and some are flaky. The Na_2SiO_3 was removed from the roasted ore by water leaching and filtration, and the

desilication residue was obtained, as shown in Fig. 5c. The composition of the desilication residue is mainly silica, with a small amount of Fe_2O_3 , mainly large particles, irregular in shape, and porous.

Figure 5d shows the micro-morphology of amorphous silica prepared by the carbonation decomposition method. The main composition is silica, which is porous and large particles are agglomerated from small particles. In the upper right corner of the figure, the physical image of amorphous silica is given, showing a bright white, fluffy granular appearance.

Phase Variation of Nickel Slag During Reduction Treatment

Figure 6a shows the XRD pattern of the nickel slag, in which it can be seen that the main phase is quartz, followed by jarosite, with small amounts of talc and serpentine.

After NaOH roasting, only a small amount of quartz remains, and other minerals either disappear or are masked by other minerals. Quartz and serpentine are converted into Na_2SiO_3 and

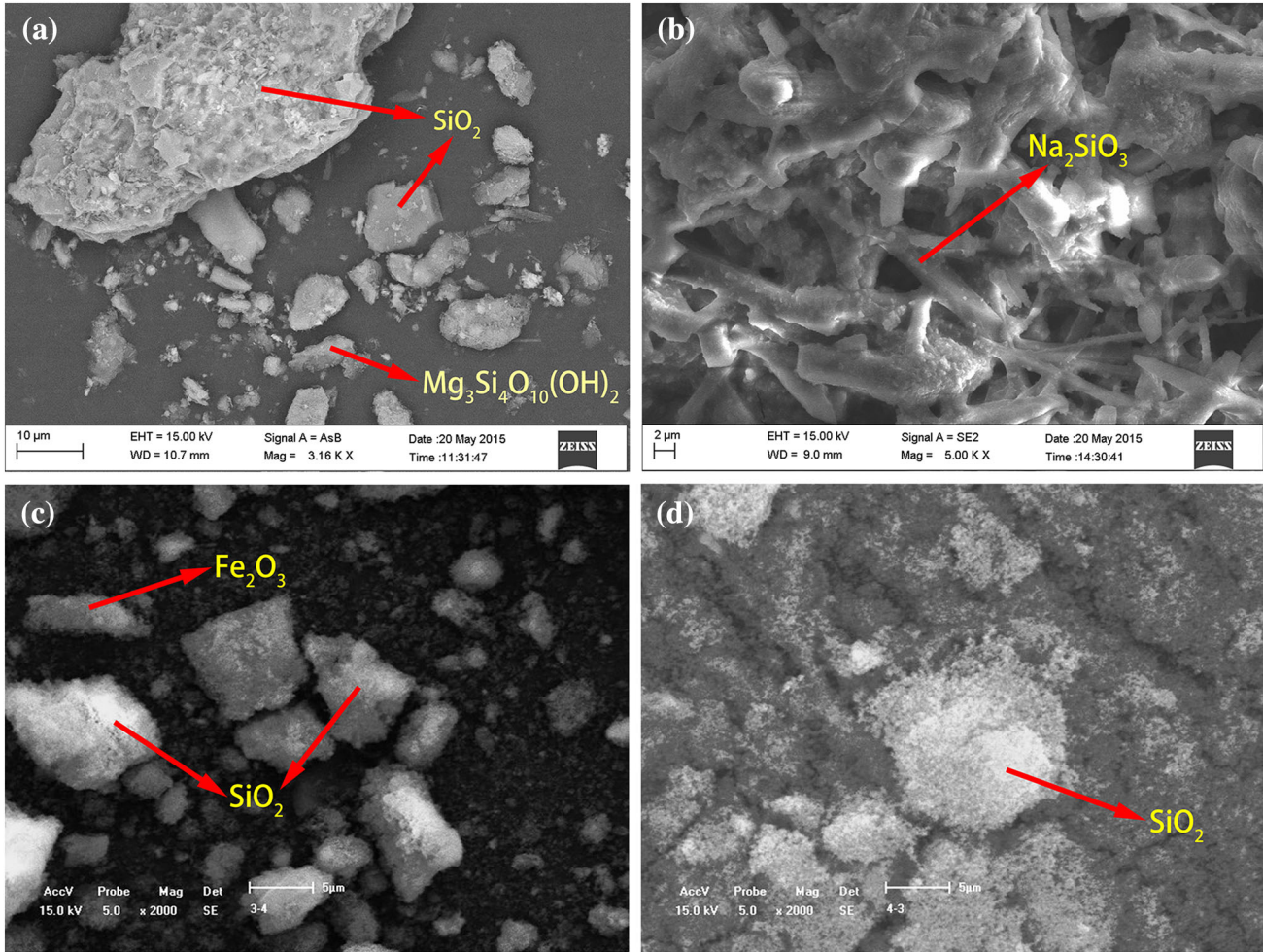
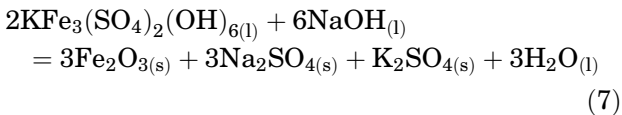
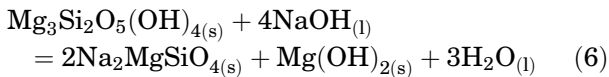


Fig. 5. SEM images of nickel slag (a), roasted ore (b), desilication residue (c), amorphous silica (d).

$\text{Na}_2\text{MgSiO}_4$ by Eqs. 1 and 6, respectively. In the disappeared phase, jarosite is converted to Fe_2O_3 by Eq. 7, while talc was not involved in the reaction. These products are masked, as shown in Fig. 6b.



Na_2SiO_3 and $\text{Na}_2\text{MgSiO}_4$ were removed from the roasted ore after water leaching and filtration, in which $\text{Na}_2\text{MgSiO}_4$ was converted into $\text{Mg}(\text{OH})_2$ by Eq. 8 and remained in the desilication residue. Quartz is still retained in the desilication residue, as shown in Fig. 6c. In the new phases, Fe_2O_3 comes from the decomposition of jarosite, and magnetite and talc are brought by the nickel slag.

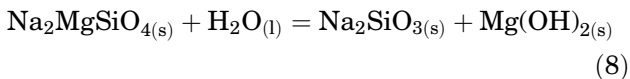


Figure 6d shows the XRD pattern of amorphous silica. In the pattern, there is no sharp crystal diffraction peak, but only a dispersed glass peak in the range of diffraction angles (2θ) 15° – 40° . This shows that the product is amorphous and does not contain other crystalline phases, so it is amorphous silica.⁴

Variation of Chemical Compositions of Nickel Slag During Reduction Treatment

In order to show more intuitively the reduction effect of nickel slag, the chemical composition of the slag and its desilication residue in Table I are compared, as shown in Fig. 7. Obviously, the content of silica decreased from 70.43% in the nickel slag to 17.65% in the filter slag, almost reducing by 75%, and the desilication ratio of silica is 91.3%, but the content of other metal oxides increased to a certain extent. Among them, Fe_2O_3 increased from 7.91% to 22.03%, and MgO from 3.74% to 10.41%. However, the amount of Al_2O_3 only increased from 2.33% to 3.38%. The reason is that some $\text{NaAl}(\text{OH})_4$ is produced by Al_2O_3 and

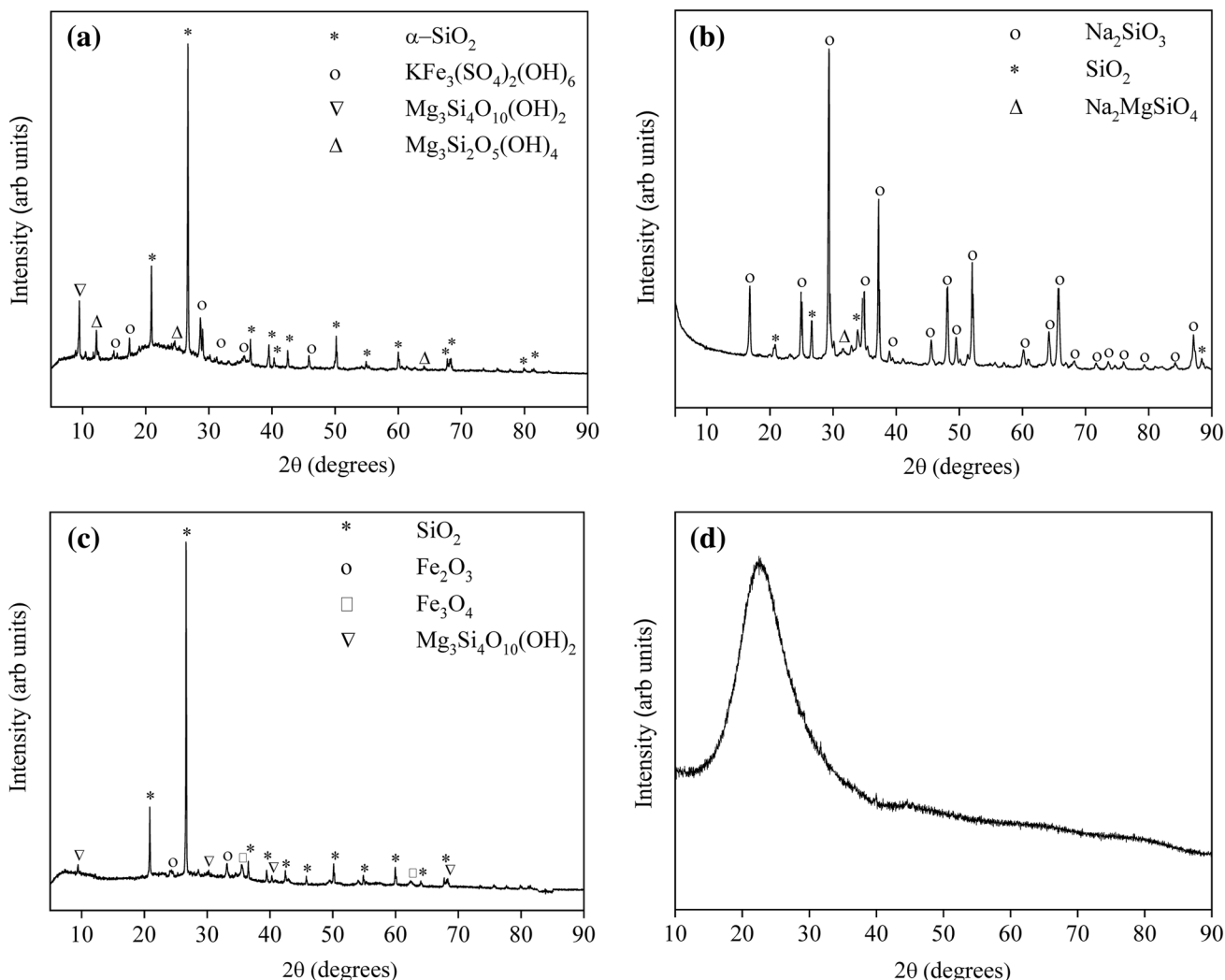


Fig. 6. XRD pattern of nickel slag (a), roasted ore (b), desilication residue (c), amorphous silica (d).

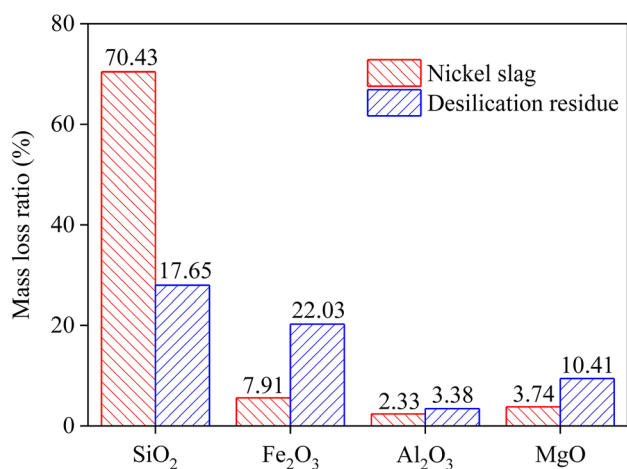


Fig. 7. Composition variations of nickel slag and its desilication residue.

enters into the Na₂SiO₃ solution, while Fe₂O₃ and MgO in nickel slag are left in the desilication residue. Thus, the desilication residue can be

further developed and utilized as a polymetallic enriched ore.

CONCLUSION

A novel alkali-saving NaOH roasting method is developed in this paper in order to carry out the reduction treatment of nickel slag. The effects of the process parameters on the weight loss ratio of the nickel slag, the carbonation decomposition time, the micro-morphology variation of the slag, the phase variation during the slag and its chemical composition variation during the reduction process are studied systematically. The following conclusions can be drawn:

1. A novel reduction treatment process for nickel slag is proposed in this paper. The desilication of the slag was completed without changing the normal operation of the original nickel extraction process.
2. The optimal process parameters of NaOH roasting are determined, i.e., the premixing time of

120 s, the roasting temperature of 823 K, the alkali–ore ratio of 1.6:1 and the roasting time of 20 min. Compared with the NaOH roasting process with stirring by Mu et al., the alkali-saving ratio is 60% for the same weight of minerals, which lowers the material burden in the reduction process. In addition, the equipment is simplified, which facilitates the realization of industrial automation.

- The optimal process parameters of carbonation decomposition are determined, i.e., the gas flow rate of 80 ml/min, the stirring speed of 450 r/min, the pH_1 of 9.95 and the first-step temperature of 333 K, and the pH_2 of 8.05 and the second-step temperature of 353 K. Amorphous silica with high purity (i.e., 99.92%) was prepared in this procedure as the final product.
- After the proposed reduction treatment, the weight loss ratio of the nickel slag is 64.1%, and the desilication ratio of the silica is 91.3%. Thus, the nickel slag is properly disposed in order to avoid environment problems and a large amount of silica resource is extracted for reuse.

The research results confirm that the proposed method is a promising way for the reduction treatment of nickel slag. On the basis of that, an environmentally friendly process route for high-silicon waste reduction has been formed. In the preliminary study, the energy consumption of this process is considered to be moderate, which is a potential advantage deserving further development.

ACKNOWLEDGEMENTS

The presented investigations have been supported by the National Basic Research Program of China (Grant No. 2007CB613603) and Project supported by National Natural Science Foundation of China (Grant No. 51774070). The authors kindly acknowledge these supports.

ELECTRONIC SUPPLEMENTARY MATERIAL

The online version of this article (<https://doi.org/10.1007/s11837-019-03914-w>) contains supplementary material, which is available to authorized users.

REFERENCES

- Y.J. Gao, H.J. Huang, W.J. Tang, X.Y. Liu, X.Y. Yang, and J.B. Zhang, *Microporous Mesoporous Mater.* 217, 210 (2015).

- J. Yang, X. Zhang, Y.Q. Liu, H.W. Ma, W.W. Feng, and C. Zeng, *Integr. Ferroelectr.* 161, 10 (2015).
- W.N. Mu, X.Y. Lu, F.H. Cui, S.H. Luo, and Y.C. Zhai, *Trans. Nonferr. Met. Soc. Chin* 28, 169 (2018).
- W.N. Mu, Doctoral dissertation (Northeastern University, 2009) (in Chinese).
- C. Li and X. Qiao, *Chem. Eng. J.* 302, 388 (2016).
- M. Iwao, M. Okuno, M. Koyano, and S. Katayama, *J. Mineral. Petrol. Sci.* 105, 135 (2010).
- Y.C. Li, X.B. Min, Y. Ke, D.G. Liu, and C.J. Tang, *Waste Manag* 83, 202 (2019).
- Y.B. Li, Z.M. Li, B. Wang, Z.M. Dong, and S.X. Song, *Miner. Eng.* 131, 376 (2019).
- T.C. Alex, P. Kumar, S.K. Roy, and S.P. Mehrotra, *Miner. Process. Extr. Metall. Rev.* 37, 1 (2016).
- A. Fedoročková, P. Raschman, G. Sučík, B. Plesingerová, Ľ. Popovič, and J. Briancin, *Ceram. -Silik.* 59, 275 (2015).
- P.L. Zhang, Z.F. Liu, T.X. Liu, and Z.Q. Li, *Eur. J. Inorg. Chem.* 32, 5577 (2014).
- C.C. Li and X.C. Qia, *Chem. Eng. J.* 302, 388 (2017).
- H.W. Guo, J. Wang, X.X. Zhang, F. Zheng, and P. Li, *Metall. Mater. Trans. B* 49, 2906 (2018).
- G.Z. Lu, T.G. Zhang, C. Cheng, W.G. Zhang, L. Wang, Y.X. Wang, and Z.M. Zhang, *Mater. Res. Express.* 6, 6 (2019).
- N.K. Mermer, M.S. Yilmaz, O.D. Oademir, and M.B. Piskin, *J. Therm. Anal. Calorim.* 129, 1807 (2017).
- K.Z. Yan, Y.X. Guo, D.D. Liu, Z.B. Ma, and F.Q. Cheng, *J. Solid State Chem.* 265, 326 (2018).
- J.N. Liu, X.Y. Shen, Y. Wu, J. Zhang, and Y.C. Zhai, *Int. J. Miner. Metall. Mater.* 23, 966 (2016).
- A. Kongnoo, S. Tontisirin, P. Worathanakul, and C. Phalakomkule, *Fuel* 193, 385 (2017).
- P.F. Fu, T.W. Yang, J. Feng, and H.F. Yang, *J. Ind. Eng. Chem.* 29, 338 (2015).
- H. Du, L. Ma, X.Y. Liu, F. Zhang, X.Y. Yang, Y. Wu, and J.B. Zhang, *Energy Fuels* 32, 5374 (2018).
- S.Q. Zhang, S. Ravi, Y.R. Lee, J.W. Ahn, and W.S. Ahn, *J. Ind. Eng. Chem.* 72, 241 (2018).
- W. Chansiriwat, D. Tanangteerapong, and K. Wantala, *Sains Malaysiana* 45, 1723 (2016).
- C. Belviso, L.C. Giannossa, F.G. Huertas, A. Lettino, A. Mangone, and S. Fiore, *Microporous Mesoporous Mater.* 212, 35 (2015).
- X.D. Wu, M.H. Fan, J.F. Mclaughlin, X.D. Shen, and G. Tan, *Powder Technol.* 323, 310 (2018).
- Y. Cheng, M.S. Xia, F. Luo, N. Li, C.B. Guo, and C.D. Wei, *Colloids Surf. A* 490, 200 (2016).
- W.B. Hu, M.M. Li, W. Chen, N. Zhang, B. Li, M. Wang, and Z.M. Zhao, *Colloids Surf. A* 501, 83 (2016).
- C.L. Liu, S.L. Zheng, S.H. Ma, Y. Luo, J. Ding, X.H. Wang, and Y. Zhang, *Fuel Process. Technol.* 173, 40 (2018).
- J. Baek, Y. Jo, J. Lee, S. Choi, and H. Jeong, *J. Nanosci. Nanotechnol.* 17, 2610 (2017).
- A. Fedoročková, P. Raschman, G. Sucik, B. Plesingerová, L. Popovic, and J. Briancin, *Ceram. -Silik.* 59, 275 (2015).
- S. Parirenyatwa, L. Escudero-Castejon, S. Sanchez-Segado, Y. Hara, and A. Jha, *Hydrometallurgy* 165, 213 (2016).
- H. Wang, Q.M. Feng, X.K. Tang, and K. Liu, *Sep. Sci. Technol.* 51, 2465 (2016).
- X.Y. Deng, Y.L. Feng, H.R. Li, Z.W. Du, J.X. Kang, and C.L. Guo, *Trans. Nonferr. Met. Soc. Chin* 28, 1045 (2018).

Publisher's Note Springer Nature remains neutral with regard to jurisdictional claims in published maps and institutional affiliations.